Acta Pharmacologica Sinica (2015) 36: 1528–1536
 1671-4083/15
www.nature.com/aps

Original Article

Preclinical pharmacokinetics of TPN729MA, a novel PDE5 inhibitor, and prediction of its human pharmacokinetics using a PBPK model

Zhi-wei GAO[1, 2], Yun-ting ZHU[2], Ming-ming YU[2], Bin ZAN[2], Jia LIU[2], Yi-fan ZHANG[2], Xiao-yan CHEN[2], Xue-ning LI[1, *], Da-fang ZHONG[2, *]

[1]*Department of Clinical Pharmacology, Zhongshan Hospital, Fudan University, Shanghai 200032, China;* [2]*Shanghai Institute of Materia Medica, Chinese Academy of Sciences, Shanghai 201203, China*

Aim: TPN729MA is a novel selective PDE5 inhibitor currently under clinical development in China for the treatment of erectile dysfunction. In this study we characterized its preclinical pharmacokinetics (PK) and predict its human PK using a physiologically based pharmacokinetic (PBPK) model.
Methods: The preclinical PK of TPN729MA was studied in rats and dogs. Human clearance (CL) values for TPN729MA were predicted from various allometric methods and from intrinsic CL determined in human liver microsomes. Human PK and plasma concentration versus time profiles of TPN729MA were predicted by using a PBPK model in GastroPlus. Considering the uncertainties in the prediction, a preliminary human study was conducted in 3 healthy male volunteers with an oral dose of 25 mg.
Results: After a single intravenous administration of TPN729MA at a dose of 1 mg/kg in rats and 3 mg/kg in dogs, the plasma CL was 69.7 mL·min^{-1}·kg^{-1} in rats and 26.3 mL·min^{-1}·kg^{-1} in dogs, and the steady-state volumes of distribution (V_{ss}) were 7.35 L/kg in rats and 6.48 L/kg in dogs. The oral bioavailability of TPN729MA was 10% in rats and above 34% in dogs. Profiles of predicted plasma concentration versus time were similar to those observed in humans at 25 mg, and the predicted T_{max}, C_{max} and AUC values were within 2-fold of the observed values.
Conclusion: TPN729MA demonstrates good preclinical PK. This compound is a valuable candidate for further clinical development. This study shows the benefits of using a PBPK model to predict PK in humans.

Keywords: TPN729MA; PDE5 inhibitor; erectile dysfunction; pharmacokinetics; human PK prediction; physiologically based pharmacokinetic model

Acta Pharmacologica Sinica (2015) 36: 1528–1536; doi: 10.1038/aps.2015.118; published online 23 Nov 2015

Introduction

Erectile dysfunction (ED) is a widespread condition that has a markedly negative impact on quality of life. This condition is strongly associated with age, and the prevalence rate of ED in men aged >40 years in China is 40%–70%[1, 2]. The physiological mechanism for achieving erection is mediated via a nitric oxide (NO)-cyclic guanosine monophosphate (cGMP) pathway[3]. The degradation of the phosphodiester bond in cGMP in arterial wall smooth muscle cells can be inhibited by phosphodiesterase type 5 (PDE5) inhibitors. PDE5 inhibitors enhance erectile function by maintaining sufficient cellular levels of cGMP in both the corpus cavernosum and the vessels supplying it, and the increasing extension of the corporeal sinusoids allows greater blood flow[4-6]. Sildenafil was the first oral PDE5 inhibitor for the treatment of ED and was approved by the US FDA in 1998. Since then, new PDE5 inhibitors such as tadalafil, vardenafil, and avanafil have been approved worldwide, and two agents (udenafil and mirodenafil) are approved only in Korea for the treatment of ED[7, 8].

TPN729MA (1-methyl-5-[2-propoxy-5-[N-methyl-N-[2-(pyrrolidin-1-yl)ethyl]] aminosulfonyl]phenyl-3-propyl-1,6-dihydro-7*H*-pyrazolo[4,3-d]pyrimidin-7-one) (Figure 1), developed by Topharman (Shanghai, China), is a novel, selective PDE5 inhibitor that is currently under clinical development in China for the treatment of ED. This compound is a potent inhibitor of human PDE5 and has a high selectivity for PDE5 compared with other known phosphodiesterases. The median inhibitory concentration (IC_{50}) of TPN729MA for PDE5 is 2.28 nmol/L, which is similar to that of tadalafil (2.35

* To whom correspondence should be addressed.
E-mail dfzhong@simm.ac.cn (Da-fang ZHONG);
li.xuening@zs-hospital.sh.cn (Xue-ning LI)
Received 2015-03-13 Accepted 2015-09-06

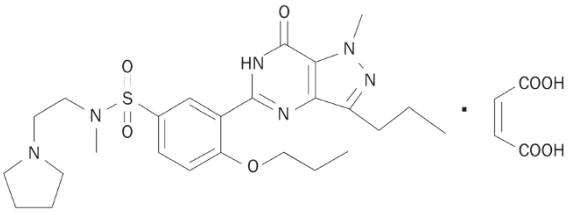

Figure 1. Chemical structure of TPN729MA.

nmol/L) and lower than that of sildenafil (5.22 nmol/L)[9]. In addition, TPN729MA significantly increases the maximum intracavernous pressure (ICP) and the ratio of ICP to blood pressure compared with vehicle in rat and dog models of erection[9].

In this article, the preclinical pharmacokinetic (PK) properties of TPN729MA were investigated after oral and intravenous administration in rats and dogs. The *in vitro* PK characteristics of TPN729MA, including Caco-2 cell permeability, plasma protein binding, blood partitioning, and hepatic microsomal metabolic stability, were also evaluated. Based on the preclinical data obtained from *in vitro* and *in vivo* systems, simulations of animal and human PK profiles for TPN729MA were performed via physiologically based pharmacokinetic (PBPK) modeling. The human PK profiles of TPN729MA were predicted to assess the likelihood that its clinical PK would support its further development as a potential therapeutic agent.

Materials and methods

Chemicals and reagents

TPN729MA (maleic acid salt, chemical purity >99%) was synthesized by Topharman (Shanghai, China). Sildenafil citrate was provided by Krka (Novo Mesto, Slovenia). High-performance liquid chromatography (HPLC)-grade methanol and acetonitrile were purchased from Sigma Aldrich (St Louis, MO, USA). HPLC-grade ammonium acetate and formic acid were purchased from Tedia (Fairfield, OH, USA). HPLC-grade water was obtained using a Milli-Q gradient water purification system (Millipore, Billerica, MA, USA).

Plasma protein binding

The extent of protein binding by TPN729MA was determined by equilibrium dialysis at two concentrations (0.2 and 2 μmol/L) in pooled Sprague–Dawley rat, beagle dog, and human plasma. TPN729MA was prepared in methanol as a stock solution and then diluted with blank plasma to achieve the test concentrations. Equilibrium dialysis was performed with a 96-well device (HTDialysis, Gales Ferry, CT, USA), in which dialysis membranes (MWCO 12–14 kDa) were incorporated after being soaked in deionized water for 60 min before use. Plasma samples (150 μL) were dialyzed against an equal volume of PBS for 16 h at 37 °C. After incubation, samples of plasma and buffer were removed and stored at −20 °C until analysis. Samples were matrix matched with blank reagents before analysis; for example, 50 μL of PBS was added to 50 μL of a plasma sample, and vice versa. Chromatographic separation was performed on an Acquity UPLC system with a BEH C_{18} column (50 mm×2.1 mm, 1.7 μm; Waters Corp, Wexford, Ireland). The column oven was set at 30 °C. The mobile phase consisted of 5 mmol/L ammonium acetate solution with 0.1% formic acid (A) and 0.1% formic acid in acetonitrile (B). A gradient elution was used with a flow rate of 0.5 mL/min. The gradient elution was 70% A, a 1.5 min linear gradient from 70% A to 10% A for 0.8 min, and an increase to 70% A for 0.5 min to re-equilibrate the column. The mass spectrometer was operated in positive ion mode with the capillary and cone voltages set at 3 kV and 10 V, respectively. The desolvation (nitrogen) gas flow rate was 1000 L/h. The desolvation temperature was 500 °C. The dwell time for each transition was 60 ms. The optimized multiple reaction monitoring (MRM) fragmentation transitions for this mode were *m/z* 517 → *m/z* 325 for TPN729MA, with a collision energy set at 30 eV. The unbound fraction (fu) of TPN729MA in plasma was calculated by dividing the concentration in the buffer by the concentration in the plasma.

Blood partitioning

The blood/plasma concentration ratio (R_{bp}) of TPN729MA was determined by incubating the compound with fresh whole blood from Sprague–Dawley rats, beagle dogs, and humans. TPN729MA was added to whole blood (final concentration 1 μmol/L), and the spiked whole blood was incubated at 37 °C for 1 h. After incubation, 50 μL aliquots of the spiked whole blood were removed, and the remaining blood was centrifuged at 2000×*g* for 10 min, after which 50 μL aliquots of plasma were removed. All of the incubations were performed in triplicate. The concentrations of TPN729MA in blood and plasma were determined by liquid chromatography–tandem mass spectrometry (LC-MS/MS) method as described above. R_{bp} was calculated by dividing the concentration in blood by the concentration in plasma after incubation.

Caco-2 cell permeability

Human colon carcinoma (Caco-2) cells, which were purchased from the American Type Culture Collection (Manassas, VA, USA), were maintained in Dulbecco's modified Eagle's medium. Caco-2 cells were cultured for 21 d in an incubator at 37 °C in a 5% CO_2 and 90% relative humidity environment. Cell layers with a transepithelial electrical resistance value of >300 Ω·cm^2 were used. Before the assay, the monolayers were gently washed three times with warm Hank's Balanced Salt Solution (HBSS; pH 7.4, 37 °C). For TPN729MA (2 μmol/L) in HBSS containing 10 mmol/L HEPES, 0.1% BSA was added to the apical side to assess permeability in the A→B direction and in the basolateral side to assess permeability in the B→A direction. The apical side and the basolateral side were maintained at pH 6.8 and 7.4, respectively. After incubation at 37 °C for 2 h, samples were collected from both the donor and receiver sides. All incubations were performed in duplicate. The concentration of TPN729MA was measured by the LC-MS/MS method described above. The apparent perme-

ability coefficient (P_{app}) was calculated using the equation P_{app} (cm/s) =[dq/dt/C_0×A], where dq/dt is the rate of permeation of the compound across the cells, C_0 is the concentration on the donor side at time 0, and A is the area of the cell monolayer. The efflux ratio (ER) was estimated as ER=$P_{app,\ B\to A}$/$P_{app,\ A\to B}$.

Metabolic stability in liver microsomes

The *in vitro* metabolic stability of TPN729MA was estimated in rat, dog, and human liver microsomes (BD Gentest, San Jose, CA, USA). All incubations were conducted in duplicate at 37 °C with a final volume of 200 μL. The incubation mixture contained TPN729MA (6 μmol/L), NADPH (1 mmol/L), and liver microsomes (rat, dog, or human, 0.5 mg protein/mL) in 100 mmol/L phosphate buffer (pH 7.4). The mixture was incubated for 3 min at 37 °C before the addition of NADPH to initiate the reaction. Incubations were quenched with 200 μL ice-cold acetonitrile at 5, 15, 30, and 60 min after the addition of NADPH.

The *in vitro* intrinsic clearance, $CL_{int,\ in\ vitro}$, was calculated from the $t_{1/2}$ of TPN729MA disappearance as $CL_{int,\ in\ vitro}$=(0.693/$t_{1/2}$)×(1/$C_{protein}$), where $C_{protein}$ is the protein concentration during the incubation, and $t_{1/2}$ was determined by the slope (k) of the log–linear regression analysis of the concentration versus time profiles; thus, $t_{1/2}$=ln2/k. The $CL_{int,\ in\ vitro}$ values were scaled to the *in vivo* values for rats, dogs, and humans by using physiologically based scaling factors, hepatic microsomal protein concentrations (47, 58, and 32 mg protein/g liver)[10], and liver weights (36.6, 32.9, and 25.7 g/kg body weight)[10]. The equation CL_{int}=$CL_{int,\ in\ vitro}$×(mg protein/g liver weight)×(g liver weight/kg body weight) was used. The *in vivo* hepatic clearance (CL_H) was then calculated by using CL_{int} and hepatic blood flow, Q (70, 40, and 20 mL·min^{-1}·kg^{-1} in rats, dogs, and humans, respectively)[11], in the well-stirred liver model disregarding all binding[12] from CL_H=(Q×CL_{int})/(Q+CL_{int}). The hepatic extraction ratio was calculated as CL_H divided by Q.

Animal PK studies

All of the animals were supplied by standard vendors in China with certificates of laboratory animal production. The animals were acclimatized at a temperature of 20 to 26 °C and relative humidity of 40%–70% under natural light/dark conditions for 2 weeks and had free access to food and water. Protocols for the care and handling of animals were in accordance with the procedures approved by the Animal Care and Use Committee of the Shanghai Institute of Materia Medica (Shanghai, China). Rats and dogs were fasted overnight and fed 2 h post dose with free access to water. TPN729MA was dissolved in saline for both intravenous and oral administration.

Male and female Sprague–Dawley rats (7–8 weeks old, 200–220 g, three males and three females in each group) were administered a single intravenous dose of 1 mg/kg or an oral dose of 1, 3, or 10 mg/kg TPN729MA. Blood samples (approximately 150 μL) were collected in heparin-coated tubes pre dose (0), and 5, 10, and 30 min, 1, 2, 4, 6, 8, 12, and 24 h post dose for intravenous dosing, and pre dose (0), and 10, 20, and 40 min, 1, 2, 4, 6, 8, 12, and 24 h post dose for oral administration. Plasma was prepared by centrifugation at 2000×*g*, and the samples were then stored at −20 °C before analysis.

Male beagle dogs (9–12 months old, 7–9 kg) were administered a single intravenous (n=3) or oral dose (n=6) of 3 or 9 mg/kg TPN729MA. Blood samples (approximately 1 mL) were collected in heparin-coated tubes pre dose (0), and 5, 10, and 30 min, 1, 2, 4, 6, 8, 12, and 24 h post dose for intravenous dosing, and pre dose (0), and 15, and 30 min, 1, 1.5, 2, 4, 6, 8, 12, and 24 h post dose for oral administration. Plasma was prepared by centrifugation at 2000×*g*, and the samples were then stored at −20 °C before analysis.

TPN729MA analysis in rat and dog plasma samples

The plasma concentration of TPN729MA was determined by protein precipitation and HPLC with mass spectrometric detection.

The plasma samples were prepared by protein precipitation. An internal standard (IS) solution (40 μL, 50.0 ng/mL sildenafil) and 50% aqueous methanol (40 μL) were added, followed by methanol (200 μL), to 40 μL of rat or dog plasma. The mixture was vortexed for 1 min and centrifuged at 11 000×*g* for 5 min. The supernatant was removed and evaporated to dryness under a flow of nitrogen at 40 °C. The residues were reconstituted in the mobile phase (100 μL), and the mixture (20 μL) was injected into the HPLC-MS/MS system for analysis.

An Agilent 1200 HPLC system equipped with a degasser, binary pump, autosampler, and thermostat-controlled column compartment (Agilent, Santa Clara, CA, USA) was used. Chromatographic separation was performed on a Zorbax SB C_{18} column (150 mm×4.6 mm, 5.0 μm, Agilent). A mixture of methanol–5 mmol/L ammonium acetate–formic acid (75:25:0.1, *v/v/v*) was used as a mobile phase at a flow rate of 0.65 mL/min. The column temperature was maintained at 30 °C. MS detection was performed on an Agilent 6460 triple-quadrupole mass spectrometer equipped with an atmospheric pressure chemical ionization (APCI) source (Agilent). The mass spectrometer was operated in the (+) APCI mode. The following MS/MS parameters were used: carrier gas temperature, 350 °C; nebulizer pressure, 20 psi; sheath gas flow, 3 L/min; sheath gas temperature, 350 °C; capillary voltage, 3000 V. Mass detection was performed in multiple reaction monitoring (MRM) mode. The optimized MRM fragmentation transition for TPN729MA was *m/z* 517 → *m/z* 325 with a collision energy of 34 V and cone voltage of 160 V. For sildenafil (IS), the optimized MRM fragmentation transition was *m/z* 475 → *m/z* 100 with a collision energy of 28 V and a cone voltage of 170 V. The scan time was 200 ms. The linear range of this method was 0.10–2000 ng/mL for TPN729MA, with a lower limit of quantification of 0.10 ng/mL.

Non-compartmental PK analysis

The plasma concentration data of TPN729MA were analyzed by non-compartmental analysis with WinNonlin software v5.3 (Pharsight Corporation, Mountain View, CA, USA). The

maximal plasma concentration (C_{max}) and the time at which the maximum concentration was reached (T_{max}) after oral administration were obtained directly from the observed data. The area under the plasma-concentration-versus-time curve from 0 to t (AUC_{0-t}) was calculated using the linear trapezoidal method and then extrapolated to infinity ($AUC_{0-\infty}$) according to the formula $AUC_{0-\infty}=AUC_{0-t}+C_{last}/\lambda_z$, where C_{last} is the plasma concentration at the last measurable time point, and the terminal phase slope (λ_z) values were determined by log–linear regression on at least three of the latest sampling time points from the plasma-concentration-versus-time curves. The elimination half-life ($T_{1/2}$) was determined as $T_{1/2}=\ln 2/\lambda_z$. After intravenous administration, the systemic plasma clearance (CL) was calculated as $CL=Dose/AUC_{0-\infty}$, and the steady-state volume of distribution (V_{ss}) was calculated as $V_{ss}=CL\times MRT$. The absolute oral bioavailability (F) was calculated as $F=(Dose_{iv}/Dose_{po})\times(AUC_{po}/AUC_{iv})\times 100\%$.

Prediction of plasma-concentration-versus-time profiles using the GastroPlus PBPK model

The GastroPlus (version 8.6; Simulations Plus, Inc, Lancaster, CA, USA) PBPK model was used for all intravenous and oral simulations in preclinical species and humans. The model has been described in detail previously[13]. Briefly, the PBPK model was composed of 14 compartments corresponding to the different tissues of the body, which were connected by the venous and arterial blood circulation. Physiological parameter values for tissue volume and blood flow were set within the software for the species of interest. The drug distribution between tissue and blood was assumed to be perfusion rate limited. The liver and kidney were considered to be the only sites of elimination.

Tissue-to-plasma partition coefficients (K_p values) were estimated using tissue composition-based methods. Two published mechanistic methods (method 1, based on Poulin and Theil[14] with the correction by Berezhkovskiy[15]; method 2, based on Rodgers *et al*[16, 17]) are available in GastroPlus for the prediction of K_p values using physicochemical and *in vitro* data such as logP and fu. The principles and assumptions of the methods have been discussed in the literature[14-17].

In addition to the species-specific physiological parameters, the observed or predicted compound-specific CL was required as an input to the model. For PBPK modeling in rats and dogs, the observed *in vivo* CL_{plasma} values obtained from a single intravenous administration of TPN729MA were used. For humans, CL values were predicted from two types of conceptually different methods, including one *in vitro*–*in vivo* extrapolation (IVIVE) method (*in vitro*), as described above, and four allometric methods (*in vivo*).

Prediction of CL from single-species allometric scaling (SSS_{rat} or SSS_{dog})

The PK profiles in rats and dogs were used to predict human CL using the equation[11] $CL_{u,\,human}=CL_{u,\,animal}\times(BW_{human}/BW_{animal})^{0.75}$, where CL_u is the unbound plasma CL (mL/min) and BW is body weight (kg), which was assumed to be 0.22 for rats, 8.4 for dogs (mean BW of the animals used in the study), and 70 for humans.

Prediction of CL using the fraction unbound intercept correction method (FCIM)

The equation $CL_{human}=33.35\ mL/min(a/R_{fu})^{0.77}$ was used[18], where the allometric coefficient (a) is obtained from the intercept of the simple allometry log–log plot between rats and dogs, and R_{fu} is the ratio of fu in rat and human plasma.

Prediction of CL using the two-species scaling method (TS) with rat-dog-human proportionality for the bound drug ($TS_{rat\text{-}dog}$)

The equation $CL_{human}=a_{(rat\text{-}dog)}\times BW_{human}^{0.628}$ was used[19], where the allometric coefficient (a) was obtained from the intercept of the simple allometric log–log plot and a fixed value of 0.628 was used as the allometric exponent.

To predict the rate and extent of the oral absorption of TPN729MA, the Advanced Compartmental Absorption Transit (ACAT) model[20] was used. The ACAT model is based on the Compartmental Absorption Transit model described by Yu and Amidon[21]. The main input parameters for the simulation were molecular weight, p*K*a, log*P*, solubility, Caco-2 permeability, R_{bp}, fu, and CL values in rats, dogs, and humans (Table 1). A preliminary human PK study was conducted with an oral dose of 25 mg TPN729MA to 3 healthy Chinese male volunteers. All subjects gave written informed consent for participation in the clinical trials. The simulated plasma-concentration-versus-time curves and the predicted PK parameters were compared with the observed human data to evaluate the accuracy of prediction.

Results

Plasma protein binding and blood/plasma ratios

The non-specific binding was negligible, and no compound instability issues were found in this study. Protein binding of TPN729MA is independent of concentration in the range of 0.2 and 2 μmol/L for all species. Therefore, a single value of fu was used for each species based on the overall mean of the data at different concentration levels. The fu of TPN729MA in rat, dog, and human plasma was 15.8%, 14%, and 10%, respectively.

Table 1. Input data used in the GastroPlus PBPK model.

Parameter	Value
Molecular weight (g/mol)	516
p*K*a	4.56
Log*P*	3.74
Caco-2 permeability (10^{-6} cm/s)	7.06
Aqueous solubility at pH 7 (mg/mL)	30
R_{bp} in rat, dog, human	1.38, 1.14, 1.06
%fu in rat, dog, human plasma	15.8, 14.0, 10.0
CL_p in rat and dog ($mL\cdot min^{-1}\cdot kg^{-1}$)	69.7, 26.3
Human CL_p predicted (from IVIVE, SSS_{rat}, SSS_{dog}, FCIM, and $TS_{rat\text{-}dog}$, $mL\cdot min^{-1}\cdot kg^{-1}$)	12.3, 10.3, 11.1, 6.42, 9.53

The mean R_{bp} of TPN729MA in rats, dogs, and humans was 1.38, 1.14, and 1.06, respectively.

Caco-2 cell permeability

TPN729MA exhibited an A→B permeability of 7.06×10^{-6} cm/s and a B→A permeability of 19.9×10^{-6} cm/s, yielding an efflux ratio of 2.82. TPN729MA displayed moderate-to-high permeability in the Caco-2 cell permeability assay.

In vitro metabolism by liver microsomes

The *in vitro* liver microsomal metabolism of TPN729MA in various species, as measured by the disappearance of TPN729MA, is summarized in Table 2. The $CL_{int,\ in\ vitro}$ of TPN729MA was 99.8, 16.6, and 33.8 $\mu L\cdot min^{-1}\cdot mg^{-1}$ protein in rat, dog, and human liver microsomes, respectively. The rate of TPN729MA metabolism in microsomes followed the order rat>human>dog. The apparent CL_{int} values of TPN729MA for rats, dogs, and humans were 172, 31.8, and 27.8 $mL\cdot min^{-1}\cdot kg^{-1}$, and the extrapolated CL_H was 49.7, 16.7, and 11.6 $mL\cdot min^{-1}\cdot kg^{-1}$, respectively. The liver microsomal turnover of TPN729MA accurately predicted (1.02-fold and 1.31-fold) the rat and dog *in vivo* CL.

Animal PK

The PK parameters of TPN729MA calculated from its concentrations in rat and dog plasma are presented in Table 3. The plasma-concentration-versus-time profiles of TPN729MA are shown in Figure 2.

After a single intravenous administration of TPN729MA at a dose of 1 mg/kg in rats and 3 mg/kg in dogs, the total plasma clearance (CL_p) was 69.7 and 26.3 $mL\cdot min^{-1}\cdot kg^{-1}$, respectively. Based on the *in vitro* R_{bp} value (1.38 and 1.14) for each species, the blood clearance (CL_b) was estimated to be 50.5 and 23.1 $mL\cdot min^{-1}\cdot kg^{-1}$ in rats and dogs, respectively. The hepatic extraction ratio (CL_b/Q_H) in rats and dogs was 72.1% and 57.8%, respectively, indicating that TPN729MA displayed moderate-to-high clearance in preclinical animals. The steady-state volume of distribution was estimated to be 7.35 and 6.48 L/kg in rats and dogs, respectively, demonstrating extensive distribution into tissues (>9 times the total body water). After a single oral administration of TPN729MA at 1, 3, and 10 mg/kg in rats, TPN729MA was absorbed with C_{max} values of 3.58, 10.7, and 44.3 ng/mL at 0.67–1 h post dose. The AUC values at 1, 3, and 10 mg/kg were 20.5, 56.1, and 207 ng·h/mL, respectively. The increases in C_{max} and AUC were roughly dose proportional. The estimated oral $T_{1/2}$ was 3.55–6.73 h. The oral absolute bioavailability was estimated to be 10% in rats. After a single oral administration of TPN729MA at 3 and 9 mg/kg in dogs, the C_{max} of TPN729MA was reached at 1.4 h post dose. The AUC values were 525 and 2763 ng·h/mL for the 3 and 9 mg/kg doses, respectively. The increases in the C_{max} and AUC were greater than dose proportional. The estimated oral $T_{1/2}$ was 3.6 h. The oral absolute bioavailability was estimated to be 34.5% and 59.4% in dogs for the 3 and 9 mg/kg doses, respectively.

PBPK modeling and human PK prediction

In this study, the PBPK model was initially optimized and validated in rats and dogs by using the obtained preclinical data. The V_{ss} values of TPN729MA predicted by using differ-

Table 2. Metabolic stability of TPN729MA in liver microsomes of different species.

Species	$t_{1/2}$ (min)	$CL_{int,\ in\ vitro}$ ($\mu L\cdot min^{-1}\cdot mg^{-1}$ protein)	CL_{int} ($mL\cdot min^{-1}\cdot kg^{-1}$)	Extrapolated CL_H ($mL\cdot min^{-1}\cdot kg^{-1}$)	Observed CL_H[a] ($mL\cdot min^{-1}\cdot kg^{-1}$)
Rat	13.9	99.8	172	49.7	50.5
Dog	83.5	16.6	31.7	17.7	23.1
Human	41.0	33.8	27.8	11.6	/

[a]Blood CL calculated from measured plasma CL and R_{bp}.

Table 3. Pharmacokinetic parameters of TPN729MA in rats and dogs after intravenous bolus and oral administration. Data are presented as the arithmetic mean±standard deviation except for T_{max} as median (range).

Species	Dosing route	Dose mg/kg	T_{max} (h)	C_{max} (ng/mL)	$AUC_{0-\infty}$ (ng·h/mL)	$t_{1/2}$ (h)	CL ($mL\cdot min^{-1}\cdot kg^{-1}$)	V_{ss} (L/kg)	F (%)
Rat	Iv (*n*=6)	1			196±16	3.36±1.96	69.7±5.7	7.35±0.75	
	Oral (*n*=6)	1	1.0 (0.33–4.0)	3.58±2.71	20.5±7.8	6.73±2.88			10.4
	Oral (*n*=6)	3	0.67 (0.17–4.0)	10.7±5.6	56.1±11.1	4.81±1.65			9.5
	Oral (*n*=6)	10	0.67 (0.33–2.0)	44.3±28.4	207±46	3.55±0.87			10.5
Dog	Iv (*n*=3)	3			1550±17	3.39±0.21	26.3±5.0	6.48±0.56	
	Oral (*n*=6)	3	1.3 (0.25–1.5)	103±23	525±153	3.96±0.48			34.5
	Oral (*n*=6)	9	1.5 (1.0–2.0)	505±229	2763±1061	3.28±0.34			59.4

ent tissue composition equations are shown in Table 4. The equation developed by Rodgers and Rowland provided the most accurate prediction of V_{ss} in rats and dogs compared with other methods. Using the V_{ss} values and the observed intravenous CL as inputs, simulation of the intravenous concentration-versus-time profiles for rats and dogs provided good approximations of the observed data (Figure 3). The oral plasma-concentration-versus-time profiles were also well simulated with the *in vitro* solubility data entered into GastroPlus (Figure 3). The predicted AUC values for TPN729MA in rats and dogs were 1.4- and 1.6-fold of the observed, respectively. Based on these results, the same V_{ss} prediction method was chosen for the human PBPK simulation.

The predicted human CL_p was 12.3 mL·min^{-1}·kg^{-1} using the *in vitro* CL_{int} determined in human liver microsomes. The human CL_p was predicted to be 10.3, 11.1, 6.42, and 9.53 mL·min^{-1}·kg^{-1} according to the SSS_{rat}, SSS_{dog}, FCIM, and $TS_{rat\text{-}dog}$ methods, respectively. No obvious differences (within 1.3-fold) in the human CL were predicted with the different prediction methods, except for FCIM. It is unclear which value provided a closer estimate of human CL prior to the first in human clinical PK study. These CL estimates were combined with the PBPK model to predict human PK profiles of TPN729MA. The proposed effective dose of TPN729MA in humans (70 kg) extrapolated from the rat efficacious dose of 2.5 mg/kg[9] based on body surface area correlation was approximately 25 mg. The human PK of TPN729MA following an oral dose of 25 mg was simulated. The predicted and observed human PK parameters and plasma concentration versus time profiles after oral administration are shown in Figure 4 and Table 5. Overall PBPK modeling reasonably matched the plasma concentration-time profiles of TPN729MA in humans. The predicted PK parameters (T_{max}, C_{max}, AUC and $T_{1/2}$) using CL values from the $TS_{rat\text{-}dog}$, SSS_{rat}, and SSS_{dog} methods were within 2-fold of the observed values. The plasma exposures of TPN729MA (AUC) were generally overpredicted using CL from FCIM (2-fold) and underpredicted using CL from HLM (1.9-fold).

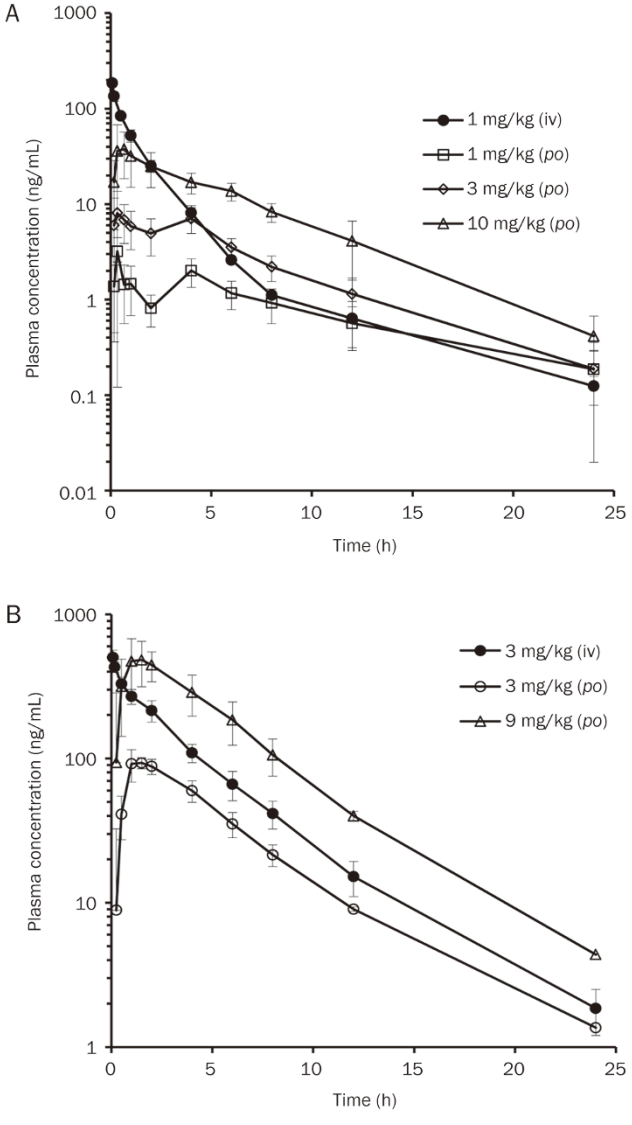

Figure 2. Plasma-concentration-versus-time profiles of TPN729MA in rats (A) and dogs (B) after intravenous (iv) or oral dose (*po*) of TPN729MA. Doses were 1 mg/kg (iv) and 1, 3 and 10 mg/kg (*po*) in rats. Doses were 3 mg/kg (iv) and 3 and 9 mg/kg (*po*) in dogs. Data are presented as the arithmetic mean±standard deviation.

Table 4. Prediction of TPN729MA V_{ss} in rat, dog and human using different mechanistic tissue composition equations.

Species	Plasma volume of distribution at steady state (L/kg)		
	Observed	Poulin & Theil	Rodgers & Rowland
Rat	7.35	7.7	6.4
Dog	6.48	14.5	7.4
Human		8.0	5.3

Discussion

TPN729MA is a novel, selective PDE5 inhibitor that is currently under clinical development for the treatment of ED. TPN729MA is a highly soluble (30 mg/mL in water) and moderately lipophilic weak base. The moderate-to-high perme-

Table 5. Predicted and observed pharmacokinetic parameters of TPN729MA in human after oral administration of TPN729MA at 25 mg. The accuracy of the prediction is expressed as fold error (the ratio of predicted to observed or observed to predicted values) in parentheses.

Simulation method	T_{max} (h)	C_{max} (ng/mL)	$AUC_{0\text{-}48}$ (ng·h/mL)	$T_{1/2}$ (h)
Observed	1.5	35.8	281	10.6
$TS_{rat\text{-}dog}$	0.84 (1.8)	54.5 (1.5)	287 (1.0)	6.4 (1.7)
SSS_{rat}	0.8 (1.9)	48.6 (1.4)	242 (1.2)	5.9 (1.8)
SSS_{dog}	0.8 (1.9)	42.8 (1.2)	203 (1.4)	5.5 (1.9)
HLM-IVIVE	0.8 (1.9)	34.3 (1.0)	152 (1.9)	4.9 (2.2)
FCIM	0.9 (1.7)	80.4 (2.2)	559 (2.0)	9.5 (1.1)

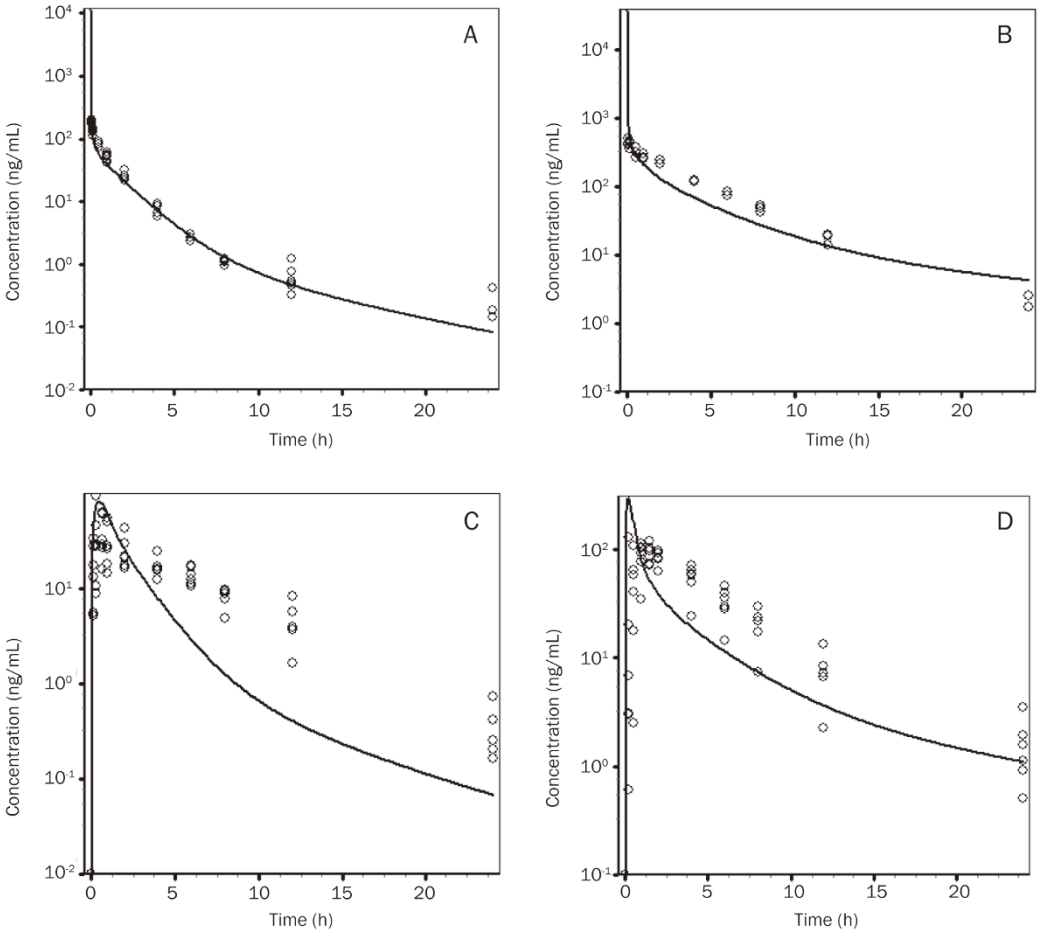

Figure 3. Observed and PBPK-model-predicted plasma-concentration-versus-time profiles of TPN729MA after intravenous administration to rats (A) or dogs (B) and oral administration to rats (C) or dogs (D). Open circles represent observed data from individual animals, and solid lines represent the profiles predicted from the PBPK model in GastroPlus. Doses were 1 mg/kg (iv) and 10 mg/kg (*po*) in rats and 3 mg/kg (iv) and 3 mg/kg (*po*) in dogs.

ability of TPN729MA in the Caco-2 assay, as well as its high solubility, suggest that it may show high intestinal absorption in humans.

With respect to hepatic blood flow, TPN729MA displays moderate-to-high clearance in preclinical animals. Systemic plasma CL in rats and dogs was converted to blood CL by using the measured blood/plasma ratio for each species. The CL in rats (72% of hepatic blood flow) was higher than that in dogs (58% of hepatic blood flow). The lower exposure in rats after oral administration is consistent with the higher CL observed after intravenous administration. There was an excellent correlation between the predicted and observed CL values (1.02-fold for rats and 1.31-fold for dogs) when the rate of *in vitro* liver microsome turnover was used to predict the *in vivo* CL in rats and dogs with physiologically based scaling factors. Based on this correlation and the fact that systemic CL was not underestimated in rats and dogs, the major route of clearance in preclinical animals is likely to be via hepatic metabolism. A mass balance study of TPN729MA after oral administration to rats showed that the elimination of the parent drug through urine and bile was negligible (<1% of the dose, data not shown), thus confirming the liver metabolic

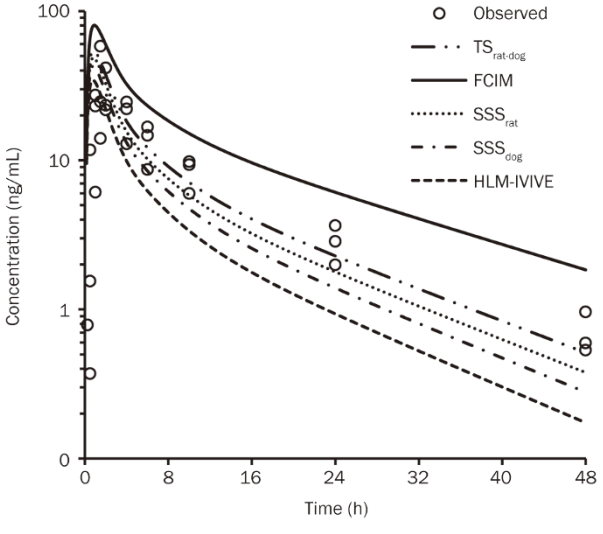

Figure 4. Predicted and observed plasma-concentration-versus-time profiles of TPN729MA after oral administration of 25 mg TPN729MA to healthy volunteers. Observed (cycle) plasma concentration time profiles were obtained from 3 healthy Chinese male subjects after a single oral administration of TPN729MA at 25 mg.

clearance of TPN729MA.

Several reports have described the utility of the PBPK method for the prediction of human pharmacokinetics[22–27]. Commercially available PBPK software, including GastroPlus (http://www.simulations-plus.com), Simcyp (http://www.simcyp.com), and PK-sim (http://www.systems-biology.com/products/pksim.html), are increasingly being used for the retrospective or prospective prediction of human PK in the pharmaceutical industry[28–33]. To simulate human PK and plasma-concentration-versus-time profiles using PBPK models, it is necessary to estimate the CL and distribution of a compound. In addition, an important component of any oral PK simulation is the predicted rate and extent of absorption[22]. Here, the human PK of TPN729MA following oral administration to humans was predicted by using available preclinical and *in vitro* data before it was administered in a human clinical study. The overall PBPK model was initially validated in rats and dogs, and it reasonably matched the rat and dog intravenous and oral plasma-concentration-versus-time profiles of TPN729MA. The predicted AUC values for TPN729MA after oral administration were within 1.6-fold of the observed values. According to the literature[31, 34], less than a twofold error was considered to be an accurate prediction using PBPK modeling.

In this article, the human CL of TPN729MA was predicted by using different methods, including IVIVE, SSS, and two of the most accurate prediction methods recommended by the PhMRA CPCC initiative[10], FCIM and $TS_{rat\text{-}dog}$. A previous retrospective analysis[11] of CL prediction methods has suggested that if CL is principally metabolized by CYP450, then human liver microsome scaling is as predictive of oral CL as SSS, based on rat, dog, and monkey data. In the present study, the *in vitro* CL (12.3 $mL{\cdot}min^{-1}{\cdot}kg^{-1}$) predicted from human liver microsomes is consistent with the CL values predicted from SSS_{rat} (10.3 $mL{\cdot}min^{-1}{\cdot}kg^{-1}$) and SSS_{dog} (11.1 $mL{\cdot}min^{-1}{\cdot}kg^{-1}$). Based on all of the available information, TPN729MA was assumed to be predominantly cleared by hepatic metabolism in humans. The CL of TPN729MA was 32% to 62% of liver blood flow in humans, based on the low CL (6.42 $mL{\cdot}min^{-1}{\cdot}kg^{-1}$) to the high CL (12.3 $mL{\cdot}min^{-1}{\cdot}kg^{-1}$), respectively. Due to the uncertainties in the prediction of the human PK profile of TPN729MA, a preliminary human study was conducted with an oral dose of 25 mg to allow an accurate estimate of PK in healthy male volunteers. In combination with the *in vitro* data, the ACTA model in GastroPlus software predicted that the C_{max} of TPN729MA was 1.0- to 2.2-fold of the observed value following oral administration of 25 mg. The predicted AUC was 1.0- to 2.0-fold of the observed value. In general, it is very difficult to know prospectively which prediction method works best for a new compound. In this study, the $TS_{rat\text{-}dog}$ method provided the most accurate PK prediction (1.0-fold for AUC and 1.5-fold for C_{max}) in humans. The SSS_{rat} and SSS_{dog} methods provided similar prediction accuracies. The prediction accuracies with FCIM and IVIVE were worse than those with $TS_{rat\text{-}dog}$, SSS_{rat} and SSS_{dog}.

Overall, the preclinical PK profiles of TPN729MA in rats and dogs were characterized by rapid absorption, moderate-to-high CL, high distribution, and low-to-moderate bioavailability. Human CL was predicted by using multiple *in vitro* and *in vivo* prediction methods. The human PK and plasma-concentration-versus-time profiles of TPN729MA were predicted using a PBPK model. A limitation of the present study was the relatively small clinical sample size. In future clinical development, this PBPK model could be refined to incorporate additional information o=n drug disposition from available clinical studies. Successful prediction of human PK profiles may result in decreased compound attrition during drug development and reduce the costs and time associated with failed clinical trials. The PBPK model could be extended to predict a wide dose range to facilitate the design of clinical studies and dose escalation procedures, as well as to explore food effects and possible drug–drug interactions.

Author contribution

Zhi-wei GAO designed the research, analyzed data, and wrote the paper; Xiao-yan CHEN, Da-fang ZHONG, and Xue-ning LI designed the research; Yun-ting ZHU, Ming-ming YU, Bin ZAN, Yi-fan ZHANG and Jia LIU performed the research.

References

1 Hong K, Xu QQ, Zhao YP, Gu YQ, Jiang H, Wang XF, *et al*. Andrology in China: current status and 10 years' progress. Asian J Androl 2011; 13: 512–8.
2 Zhang K, Xu B, Liu D, Wang X, Zhu J, Deng C, *et al*. Sildenafil improves erectile hardness in Chinese men with erectile dysfunction: a real-life study analyzed on age stratification. Urology 2014; 83: 831–6.
3 Gupta M, Kovar A, Meibohm B. The clinical pharmacokinetics of phosphodiesterase-5 inhibitors for erectile dysfunction. J Clin Pharmacol 2005; 45: 987–1003.
4 Francis SH, Corbin JD. Molecular mechanisms and pharmacokinetics of phosphodiesterase-5 antagonists. Curr Urol Rep 2003; 4: 457–65.
5 Corbin JD, Francis SH. Pharmacology of phosphodiesterase-5 inhibitors. Int J Clin Pract 2002; 56: 453–9.
6 Rezvanfar MA, Rahimi HR, Abdollahi M. ADMET considerations for phosphodiesterase-5 inhibitors. Expert Opin Drug Metab Toxicol 2012; 8: 1231–45.
7 Bruzziches R, Francomano D, Gareri P, Lenzi A, Aversa A. An update on pharmacological treatment of erectile dysfunction with phosphodiesterase type 5 inhibitors. Expert Opin Pharmacother 2013; 14: 1333–44.
8 Bell AS, Palmer MJ. Novel phosphodiesterase type 5 modulators: a patent survey (2008-2010). Expert Opin Ther Pat 2011; 21: 1631–41.
9 Wang Z, Zhu DF, Yang XC, Li JF, Jiang XR, Tian GH, *et al*. The selectivity and potency of the new PDE5 inhibitor TPN729MA. J Sex Med 2013; 10: 2790–7.
10 Ring BJ, Chien JY, Adkison KK, Jones HM, Rowland M, Jones RD, *et al*. PhRMA CPCDC initiative on predictive models of human pharmacokinetics, part 3: Comparative assessment of prediction methods of human clearance. J Pharm Sci 2011; 100: 4090–110.
11 Hosea NA, Collard WT, Cole S, Maurer TS, Fang, RX, Jones HM, *et al*. Prediction of human pharmacokinetics from preclinical information: comparative accuracy of quantitative prediction approaches. J Clin Pharmacol 2009; 49: 513–33.

12 De Buck SS, Sinha VK, Fenu LA, Gilissen RA, Mackie CE, Nijsen MJ. The prediction of drug metabolism, tissue distribution, and bioavailability of 50 structurally diverse compounds in rat using mechanism-based absorption, distribution, and metabolism prediction tools. Drug Metab Dispos 2007; 35: 649–59.
13 Jones HM, Parrott N, Jorga K, Lave T. A novel strategy for physiologically based predictions of human pharmacokinetics. Clin Pharmacokinet 2006; 45: 511–42.
14 Poulin P, Theil FP. Prediction of pharmacokinetics prior to *in vivo* studies. 1. Mechanism-based prediction of volume of distribution. J Pharm Sci 2002; 91: 129–56.
15 Berezhkovskiy LM. Volume of distribution at steady state for a linear pharmacokinetic system with peripheral elimination. J Pharm Sci 2004; 93: 1628–40.
16 Rodgers T, Leahy D, Rowland M. Physiologically based pharmacokinetic modeling 1: predicting the tissue distribution of moderate-to-strong bases. J Pharm Sci 2005; 94: 1259–76.
17 Rodgers T, Rowland M. Physiologically based pharmacokinetic modelling 2: predicting the tissue distribution of acids, very weak bases, neutrals and zwitterions. J Pharm Sci 2006; 95: 1238–57.
18 Tang H, Mayersohn M. A novel model for prediction of human drug clearance by allometric scaling. Drug Metab Dispos 2005; 33: 1297–303.
19 Tang H, Hussain A, Leal M, Mayersohn M, Fluhler E. Interspecies prediction of human drug clearance based on scaling data from one or two animal species. Drug Metab Dispos 2007; 35: 1886–93.
20 Agoram B, Woltosz WS, Bolger MB. Predicting the impact of physiological and biochemical processes on oral drug bioavailability. Adv Drug Deliv Rev 2001; 50: S41–67.
21 Yu LX, Amidon GL. A compartmental absorption and transit model for estimating oral drug absorption. Int J Pharm1999; 186: 119–25.
22 Allan G, Davis J, Dickins M, Gardner I, Jenkins T, Jones H, *et al*. Pre-clinical pharmacokinetics of UK-453,061, a novel non-nucleoside reverse transcriptase inhibitor (NNRTI), and use of in silico physiologically based prediction tools to predict the oral pharmacokinetics of UK-453,061 in man. Xenobiotica 2008; 38: 620–40.
23 Bungay PJ, Tweedy S, Howe DC, Gibson KR, Jones HM, Mount NM. Preclinical and clinical pharmacokinetics of PF-02413873, a nonsteroidal progesterone receptor antagonist. Drug Metab Dispos 2011; 39: 1396–405.
24 Yamazaki S, Skaptason J, Romero D, Vekich S, Jones HM, Tan W, *et al*. Prediction of oral pharmacokinetics of cMet kinase inhibitors in humans: physiologically based pharmacokinetic model versus traditional one-compartment model. Drug Metab Dispos 2011; 39: 383–93.
25 Xia B, Heimbach T, He H, Lin TH. Nilotinib preclinical pharmacokinetics and practical application toward clinical projections of oral absorption and systemic availability. Biopharm Drug Dispos 2012; 33: 536–49.
26 Liu F, Zhuang XM, Yang CP, Li Z, Xiong S, Zhang ZW, *et al*. Characterization of preclinical *in vitro* and *in vivo* ADME properties and prediction of human PK using a physiologically based pharmacokinetic model for YQA-14, a new dopamine D3 receptor antagonist candidate for treatment of drug addiction. Biopharm Drug Dispos 2014; 35: 296–307.
27 Li GF, Wang K, Chen R, Zhao HR, Yang J, Zheng QS. Simulation of the pharmacokinetics of bisoprolol in healthy adults and patients with impaired renal function using whole-body physiologically based pharmacokinetic modeling. Acta Pharmacol Sin 2012; 33: 1359–71.
28 Jones HM, Gardner IB, Collard WT, Stanley PJ, Oxley P, Hosea NA, *et al*. Simulation of human intravenous and oral pharmacokinetics of 21 diverse compounds using physiologically based pharmacokinetic modelling. Clin Pharmacokinet 2011; 50: 331–47.
29 Jones HM, Dickins M, Youdim K, Gosset JR, Attkins NJ, Hay TL, *et al*. Application of PBPK modelling in drug discovery and development at Pfizer. Xenobiotica 2012; 42: 94–106.
30 Sinha VK, Snoeys J, Osselaer NV, Peer AV, Mackie C, Heald D. From preclinical to human-prediction of oral absorption and drug-drug interaction potential using physiologically based pharmacokinetic (PBPK) modeling approach in an industrial setting: a workflow by using case example. Biopharm Drug Dispos 2012; 33: 111–21.
31 De Buck SS, Sinha VK, Fenu LA, Nijsen MJ, Mackie CE, Gilissen RA. Prediction of human pharmacokinetics using physiologically based modeling: a retrospective analysis of 26 clinically tested drugs. Drug Metab Dispos 2007; 35: 1766–80.
32 Poulin P, Jones R, Jones HM, Gibson CR, Rowland M, Chien JY, *et al*. PHRMA CPCDC initiative on predictive models of human pharmacokinetics, part 5: Prediction of plasma concentration-time profiles in human by using the physiologically-based pharmacokinetic modeling approach. J Pharm Sci 2011; 100: 4127–57.
33 Chen Y, Jin JY, Mukadam S, Malhi V, Kenny JR. Application of IVIVE and PBPK modeling in prospective prediction of clinical pharmacokinetics: strategy and approach during the drug discovery phase with four case studies. Biopharm Drug Dispos 2012; 33: 85–98.
34 Jones HM, Gardner IB, Watson KJ. Modelling and PBPK simulation in drug discovery. AAPS J 2009; 11: 155–66.